Chemical Society Reviews

Review Article

Application of Computational Methods to the Design and Characterisation of Porous Molecular Materials

Jack D. Evans,*[a] Kim E. Jelfs,[b] Graeme M. Day[c] and Christian J. Doonan*[d]

Received 00th January 20xx,
Accepted 00th January 20xx

DOI: 10.1039/x0xx00000x

www.rsc.org/

Composed from discete units, porous molecular materials (PMMs) possess unique properties not observed for conventional, extended, solids, such as solution processibility and permanent porosity in the liquid phase. However, identifying the origin of porosity is not a trivial process, especially for amorphous or liquid phases. Furthermore, the assembly of molecular components is typically governed by a subtle balance of weak intermolecular forces that makes structure prediction challenging. Accordingly, in this review we canvass the crucial role of molecular simulations in the characterisation and design of PMMs. We will outline strategies for modelling porosity in crystalline, amorphous and liquid phases and also describe the state-of-the-art methods used for high-throughput screening of large datasets to identify materials that exhibit novel performance characteristics.

1. Introduction

Porous solids continue to be an active field of fundamental and applied research.[1,2] Due to their large surface-to-volume ratios they have found applications in areas such as separation science and catalysis.[3,4] The majority of porous materials are extended solids and examples range from amorphous (e.g. porous carbons) to highly crystalline (e.g. metal—organic frameworks (MOFs) and zeolites), in nature. [2,5,6] However, porosity is also known for solids comprised of discrete molecules.[7-9] The first examples of such materials achieved accessible porosity through interconnected pore networks that were formed via solid-state packing effects.[10,11] Subsequently, the gas adsorption properties of a number of other organic and inorganic molecules were explored (e.g. calixarenes, curcubiturils and phthalocyanines) and yielded important fundamental knowledge about the origin of porosity in molecular materials.[9] Interest in the field of PMMs burgeoned upon the report of a highly porous solid comprised of entirely organic cage molecules.[12] This work showed that the cage-based solids could afford physical adsorption properties, e.g. gas uptake and adsorption kinetics, comparable to conventionally porous materials. In addition, in contrast to extended solids these materials could be solution processed which is a desirable property for the fabrication of composite materials such as mixed matrix polymer membranes.[13,14] In addition, discrete cage molecules can be assembled via a modular synthetic approach providing a facile pathway to

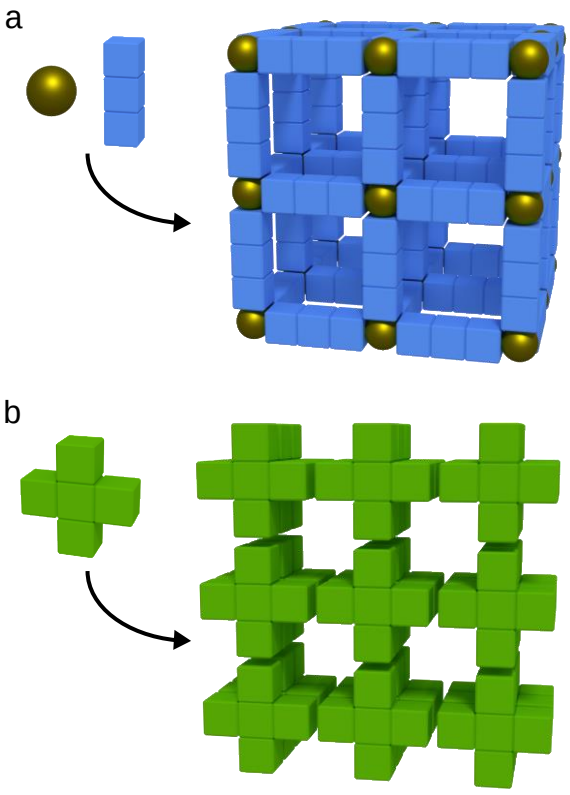

Fig. 1 (a) Conventional porous solids are comprised of an extended network of robust bonds. (b) In contrast, porous molecular solids are constructed from relatively weak intermolecular interactions between discrete molecular units.

[a] *Chimie ParisTech, PSL Research University, CNRS, Institut de Recherche de Chimie Paris, 75005 Paris, France.*
[b] *Department of Chemistry, Imperial College London, South Kensington, London SW7 2AZ, United Kingdom.*
[c] *Computational Systems Chemistry, School of Chemistry, University of Southampton, Highfield, Southampton SO17 1BJ, United Kingdom*
[d] *School of Physical Sciences, The University of Adelaide, Adelaide, South Australia 5005, Australia.*

† Footnotes relating to the title and/or authors should appear here.
Electronic Supplementary Information (ESI) available: [details of any supplementary information available should be included here]. See DOI: 10.1039/x0xx00000x

multifunctional materials.[15] In recent years our fundamental understanding of PMMs has developed. However, significant challenges remain with respect to the materials design, structure prediction and describing porosity in non-crystalline systems.

The molecular components of PMMs can possess intrinsic voids, such as cage architectures, or be inherently non-porous but realise an interconnected pore network via solid-state packing effects.[10,16] Analogous to extended solids, molecular materials can reach surface areas in excess of 3000 $m^2 g^{-1}$.[16] Furthermore, porosity is not limited to the crystalline state, with several examples of amorphous structures reported that exhibit high surface areas.[17] Indeed, recent work has shown that judicious design of cage molecules can also yield PMMs that can be described as permanently porous liquids.[18]

Compared to extended solids, such as MOFs, that are constructed from highly directional, thermodynamically, robust bonds, molecular materials are assembled via relatively soft intermolecular forces as depicted in Fig. 1. Accordingly, the energetic difference between distinct polymorphs for a given material can fall within a few $kJ.mol^{-1}$.[19] This key difference gives rise to challenges associated with the intuitive design and characterisation of PMMs. For example, bulk solids composed of intrinsically porous cage molecules are commonly non-porous due to the numerous, energetically accessible, packing arrangements that obstruct connectivity between their pore voids.[20] Additionally, the concept of 'reticular chemistry', exemplified for some MOF materials,[21] is yet to be fully realised for PMMs.[22] This can be attributed to the complex relationship between the structure and chemical functionality of the molecular building units, examples of which are illustrated in Fig. 2, and the intermolecular packing

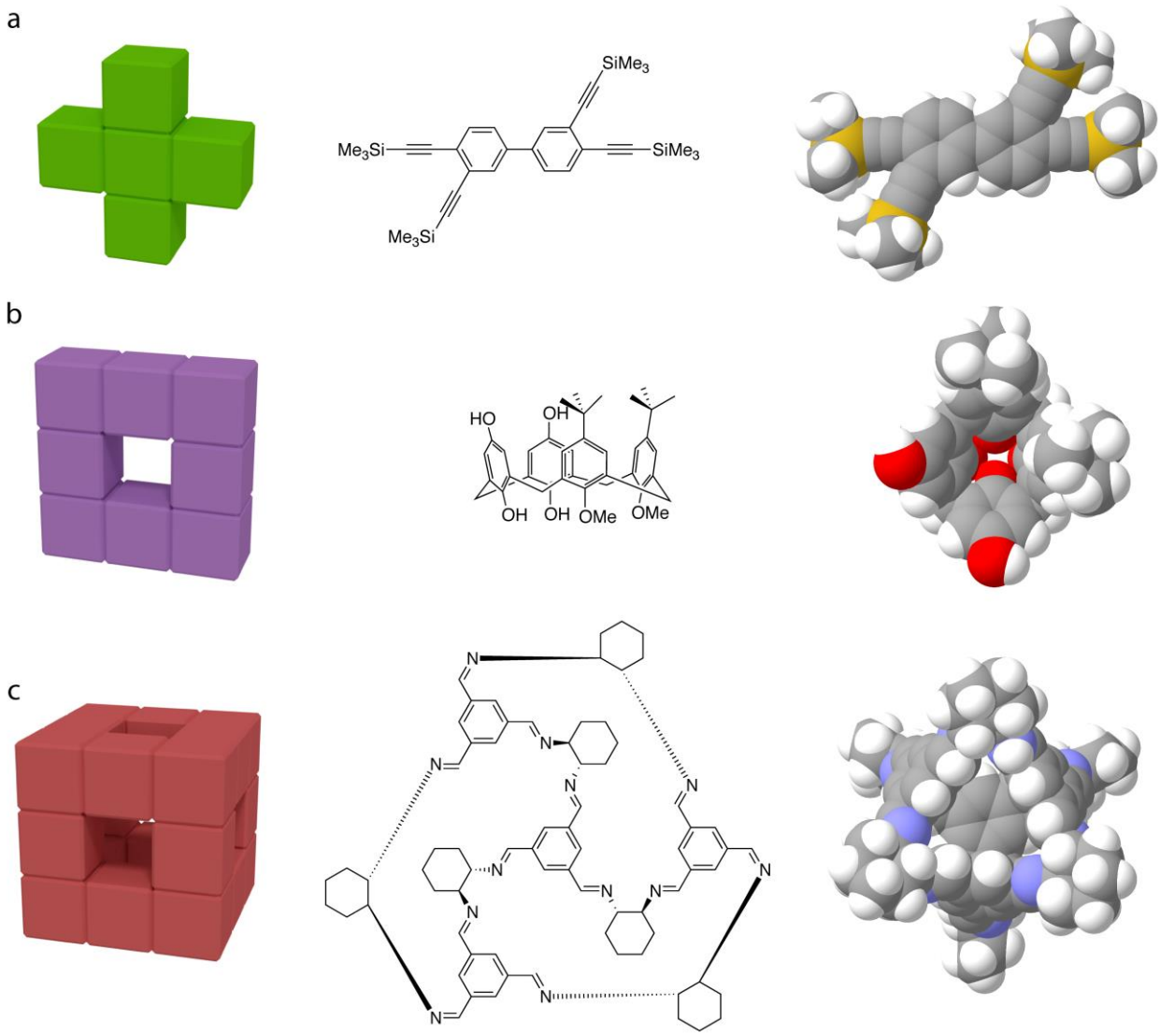

Fig. 2 Examples of molecules that exhibit permanent porosity. (a) Extrinsic porosity, observed for materials that possess no molecular voids e.g. tetra(trimethylsilylethynyl)biphenyl. (b and c) Intrinsic porosity, which is realized for macrocyclic and cage structures that possess intrinsic voids that can be interconnected in the solid state, e.g. 1,2-dimethoxyp-tert-butylcalix[4]dihydroquinone and Covalent Cage 3 (**CC3**).

forces that determine their spatial organisation in the bulk material. Characterising the origin of porosity (i.e intrinsic, extrinsic or a combination of both) in PMMs also presents a significant challenge. For example, by modifying processing methods, amorphous phase PMMs can be accessed that preclude analysis by the conventional approach of X-ray diffraction. To this end the use of computational methods has proved essential to understanding these structures.[23]

As with conventional framework materials, PMMs can be described using quantum mechanical methods including density functional theory (DFT).[24] These methods are, potentially, highly accurate, as long as care is taken to properly account for dispersion interactions,[25,26] and can elucidate geometric and energetic properties resulting from the molecular electronic structure. Alternatively, structures can be simulated using model potentials, which are less computationally demanding than quantum mechanical methods.[27] Modern model potentials (force fields) can show similar accuracy to DFT methods[28] but allow for the simulation of large systems and long timescales, which is particularly crucial for gas diffusion and adsorption. Nevertheless, accurate potential parameters or force fields are required for classical simulations which can necessitate significant investment.[29] The scope of computational methods in the field of PMMs goes beyond structural simulations and straightforward porosity analysis. For example, recent studies have shown how *in silico* approaches can be used to screen large databases for crystal structures and identify candidates that possess properties that would indicate permanent porosity.[30] In addition, crystal structure prediction algorithms have afforded significant steps towards rationalising empirical data and show promise for the design of new functional materials.[31,32]

This review will cover the application of computational approaches to the research of PMMs. In particular, simulations that produce structural models of these materials in crystalline, amorphous and liquid states will be canvassed and the novel methods of modelling porosity and gas adsorption in these systems will be discussed. Although the field of PMMs encompasses inorganic molecules and metal organic polyhedra, computational studies have largely focused on organic materials. As a consequence organic PMMs are the focus of this review, although most of the methods that are described can be adapted for studies of inorganic molecular materials.

2. Structural models

Structural models of PMMs are a vital tool for understanding their porosity. PMMs span crystalline, amorphous and liquid states, (Fig. 3) and for each of these computational methods have been employed to generate atomistic structural representations. Such models have been used to afford fundamental insight to experimental properties or to screen and predict the porosity of hypothetical molecules.[31,32]

2.1 Crystalline phase

Growing large single crystals suitable for X-ray diffraction studies is a common issue for many fields of chemistry. Furthermore, even if the appropriate conditions for crystallisation are uncovered, many crystalline polymorphs may exist, each of which can exhibit very different properties. With respect to 'porous' crystals, significant variation in surface area, pore size distribution and pore network dimensionality can be observed for different polymorphs. Moreover, the degree of crystallinity can also result in drastic variation of properties, such as surface area.[17] Accordingly, predicting the possible crystal structures from a given molecular building block is an important challenge.[33]

Methods for the prediction of crystal structures using the molecular diagram as the sole input have been developed over

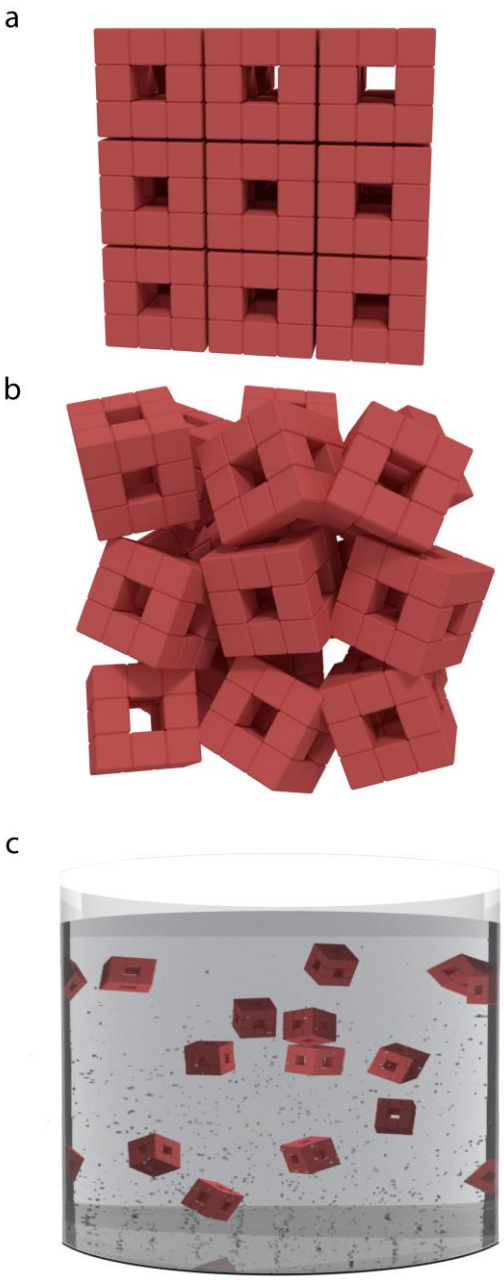

Fig. 3 A stylistic representation of the states of matter that PMMs can adopt and retain porosity: (a) crystal, (b) amorphous solid and (c) liquid.

the past few decades. As the prevalence of polymorphism has become better understood, the aims of crystal structure prediction (CSP) methods have moved on from prediction of "the" crystal structure of a molecule to the prediction of what stable crystal structures are possible and the relative thermodynamic stability of these putative polymorphs.

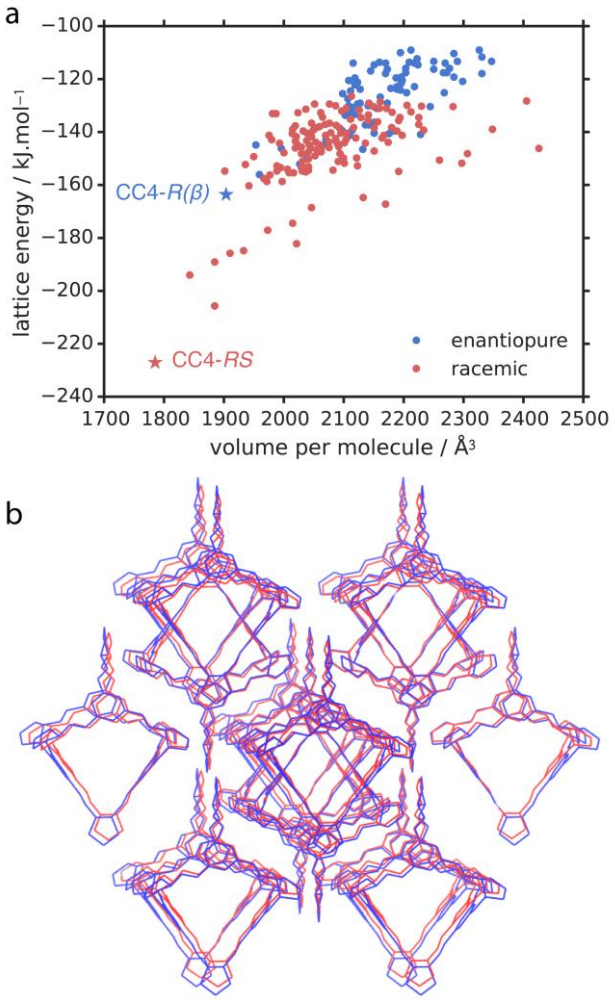

Fig. 4 (a) Crystal energy landscape simulated for cage molecule **CC4**. Here, the lowest energy structures for both the enantiopure and racemic compositions correspond to the experimentally observed structures as labelled. (b) Overlay of the experimental crystal structure of **CC4**-RS (red) and predicted crystal structure (blue). Reproduced from Ref. 20 with permission from the Royal Society of Chemistry.

Any observable crystal structure must correspond to a local minimum on the lattice energy surface. Therefore, the predominant method in CSP is to perform a global exploration of the lattice energy surface to locate all low energy local minima. In practise, this requires a method for exploring the structural phase space of possible structures, combined with a model for calculating the lattice energies of trial structures. A wide variety of approaches have been implemented for the structure searching aspect of CSP, including random and quasi-random sampling of the structural degrees of freedom (unit cell dimensions, molecular positions and orientations, and intramolecular, conformational degrees of freedom), variations on Monte Carlo simulated annealing and genetic algorithms.[34] All of these methods have been shown to be successful and the choice of search method does not seem to be crucial, so long as a sufficiently exhaustive search is performed to locate all local energy minima, including the consideration of all likely space group symmetries. What is consistent between methods is the need to perform calculations on many thousands of trial structures to fully explore the lattice energy landscape.[35]

The final list of possible crystal structures is usually ranked using their calculated lattice energies, under the assumption that the lowest energy computer-generated structures are the most likely to be observed experimentally, illustrated in Fig. 4. Hence, the success of this ranking relies on the quality of the energy model used to evaluate lattice energies. The challenge of correctly ranking crystal structures is clear from an understanding of typical energy differences between polymorphs, which is usually below 2 kJ mol^{-1}.[19] Indeed, CSP studies on organic molecules very often lead to crowded predicted energy landscapes where candidate crystal structures are separated by fractions of a kJ mol^{-1}.[36,37] A variety of energy models have been applied in CSP of molecular crystals. Early attempts made use of simple force field methods, due to their widespread use in molecular modelling and as the most affordable way of assessing the large numbers of structures that must be assessed in CSP. However, it was found early in the development and evaluation of CSP methods that the transferable force fields with simple forms for atom-atom interactions do not result in reliable, successful predictions.[38] Therefore, CSP has led to the development of more elaborate force field methods[39] and, in recent years, the availability of large scale parallel computing has enabled solid state DFT methods to be applied to CSP, with considerable success.[40]

Two of the key current challenges in CSP relate to applications to large and flexible molecules and further improvements to energy models to increase the reliability of predictions. The molecular cages developed for PMMs are much larger than most of the molecules to which CSP has been applied. The size of these molecules, and the resulting unit cells of predicted structures, put these systems out of the range of solid state DFT calculations. Therefore, force field methods are still the main method in CSP applied to porous materials. Improvements to the energy models used in CSP include a recent move towards calculating relative free energies, rather than static lattice energies.[28,41,42] The energetic contribution to polymorph free energy differences from lattice vibrations has been shown to be potentially important in recent large-scale studies, re-ranking approximately 10% of observed polymorph pairs at room temperature compared to temperature-free lattice energy rankings.[19,43] Large potential density differences between porous and non-porous packings of molecules are expected to make entropy differences important in assessing relative stabilities of predicted structures for PMMs.

A CSP challenge that is specific to PMMs is how to incorporate the templating influence of solvent inclusion in

porous crystal structures into their energetic evaluation. CSP on PMMs has to date been based on the calculated energies of unsolvated predicted crystal structures. This approach ignores the energetic contribution of included solvent molecules during crystallisation; the energetic ranking of fully solvated crystal structures may well differ from that of the unsolvated structures. It would be challenging to include solvent from the start of the CSP process, as the extent of solvent loading is unknown until the porosity of the crystal structures is predicted. The success of CSP applied to some cage molecules is probably due to the unusually large lattice energy differences between the lowest energy predicted crystal structures;[20] therefore, the differences in stabilisation due to solvation of the pores is probably smaller than the lattice energy differences themselves. However, the application of CSP to PMMs that lack such large energy differences between possible crystal structures will require the development of methods for assessing the impact of solvent inclusion during crystallisation, such as adding solvent into the pores of predicted structures up to the point where no further energetic stabilisation is achieved. [44]

Despite the need for further method development, the small number of applications of CSP to PMMs has shown the potential of these methods in this area. Jones and co-workers demonstrated that the crystal packing of a series of chiral molecular cages was predictable with high accuracy.[20,31] In the case of the enantiomerically pure organic cage **CC4**-*R*, the observed crystal structure did not correspond to the lowest energy predicted structure. However, subsequent screening of crystallisation conditions led to a new polymorph, obtained by desolvation of a *p*-xylene **CC4** solvate; the new polymorph was identified as corresponded to the lowest energy predicted crystal structure,[20] demonstrating the value of CSP in anticipating polymorphs of known molecules.

In addition to predicting their structures, the CSP results also successfully predicted the strong preference for racemic crystal packing in **CC3** and **CC4**, Fig. 4. The opposite behaviour of a large cage, **CC5**, where chiral resolution is observed during crystallisation, is in agreement with the predicted lower energy of enantiomerically pure crystal structures of **CC5** relative to the lowest energy predicted racemate. CSP was also applied to successfully predict the crystal packing when two different cage molecules were co-crystallised. The geometric accuracy of the predictions in these examples demonstrates the possibility to predict surface areas, void connectivity and pore size distributions starting from the only the molecular diagram. Hence, there is potential to use these methods to screen molecules for their promise as PMMs in advance of their synthesis. CSP has also recently been applied to understanding the structure-directing interactions in a series of tubular cage molecules; in this case, the size and flexibility of the molecules, as well as probable effects of solvent inclusion in the pores, precluded definitive structure prediction.[22] However, the calculated energy landscapes of crystal structures provided valuable information on preferred intermolecular interactions that could be applied to the design of cage co-crystals with novel pore networks.

An interesting further area for applying CSP to PMMs is in understanding and anticipating extrinsic porosity in molecular crystals. Extrinsic porosity arises due to molecular packing that leaves free space between molecules. The energy landscapes of predicted molecular crystals almost always favour close packing in the lowest energy structures. However, Cruz-Cabeza and co-workers demonstrated that the observed frameworks of inclusion crystals are also located on predicted crystal energy landscapes, at higher energies, but along the low-energy edge of energy-density distribution of crystal structures.[45] The identification of stable, low density structures among CSP structures has the promise of predicting clathrate structures,[46] but also of desolvatable extrinsically porous crystals.

Indeed, CSP was recently used to computationally assess a series of awkwardly-shaped benzimidazolones and imides for likely porous structures, finding that some molecules featured ‘spikes’ of unusually low energy structures in the low density region of their structural landscapes.[40] The results prompted experimental crystallisation screening of one of the molecules, triptycenetrisbenzimidazolone, for which an extrinsically porous structure has already been reported.[47] These screens led to the discovery of three new extrinsically porous polymorphs of the molecule, two of which corresponded to the lowest energy structures in the spikes that had been observed in the CSP landscape. One of these polymorphs has a lower density (0.41 g cm^{-3}) than any molecular solid previously reported in the Cambridge Structural Database. This work[32] also demonstrated how the usual structure-energy landscapes resulting from CSP can be augmented by simulated properties of each predicted structure, giving energy-structure-function maps that could be used to guide the discovery of porous materials with targeted properties, such as high gas storage capacity or the ability to separate mixtures of molecules.

2.2 Amorphous phase

Crystal structure data provides fundamental insight into the pore architectures of PMMs; however, in cases where the material is isolated as an amorphous phase, identifying the origin of porosity not trivial. This is especially true for cage molecules where the measured porosity can arise from connected pore voids (intrinsic porosity) or from free space existing between the molecular building units (extrinsic porosity) or a combination of both.[9] Indeed, the complexity of characterizing disordered systems is highlighted by examples where amorphisation of PMMs can give rise to increased porosity and others where disturbing a well ordered pore network leads to a bulk solid with a considerably lower porosity.[15,48,49] The inherent difficulty in understanding the pore networks of such materials has made molecular simulations that yield realistic structural representations of amorphous systems indispensable for the characterisation of PMMs.

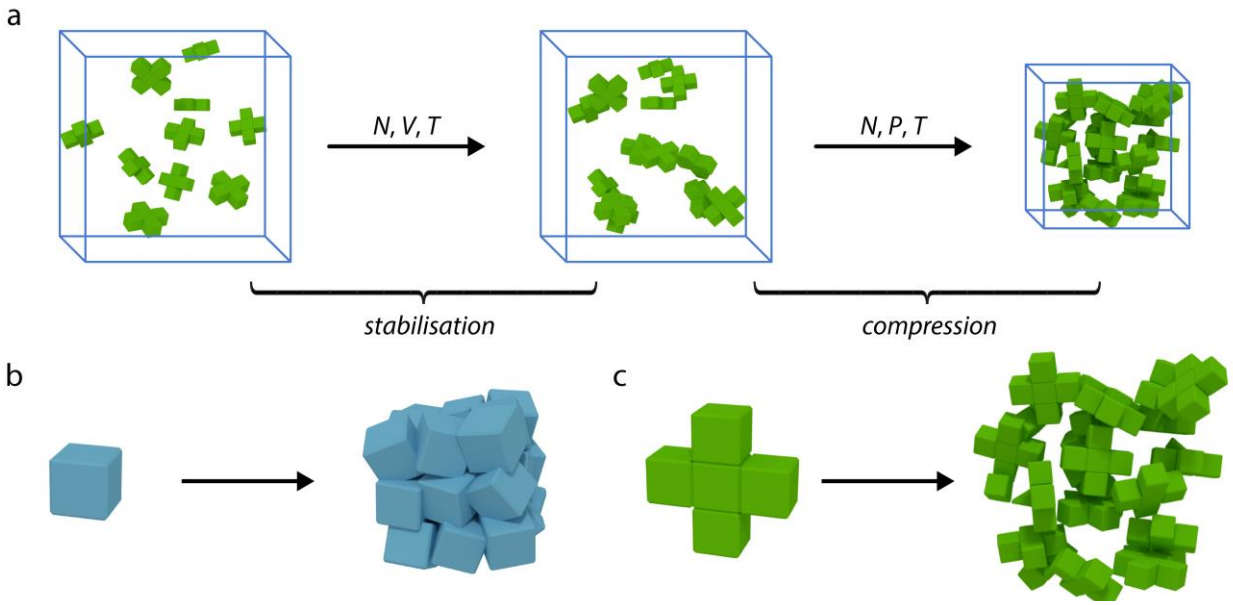

Fig. 5 (a) The key simulation steps used for the production of amorphous PMM structures. Choice of periphery functionality has been shown to significantly affect the resulting amorphous structure with (b) compact functionality leading to a dense non-porous structure and (c) bulky functionality producing a porous structure.

Amorphous systems such as polymers[50] and activated carbon,[51] have been extensively modeled. For materials composed of rigid structures, stochastic approaches, such as Monte Carlo[52] and reverse Monte Carlo[53] simulations, have been used to produce accurate structural representations.[54] However, for more complex structures, extensive molecular dynamics simulations are employed.[55] By changing atomic positions of an initial configuration by a stochastic procedure, reverse Monte Carlo uses the Metropolis algorithm[27] to test changes to the configuration on the basis of agreement between a simulated property and an experimental target, which is often density. These methods have been applied to discrete molecular carbon plates, in which the resulting systems serve as a model of extended carbon structures.[56-58] Generally, porous polymeric systems exhibit a large range of conformations, owing to uncorrelated rotation of the repeating units of the polymer.[59] Thus, the production of structural models require additional relaxation and annealing steps subsequent to initial random packing. This complication has led to the development of complex procedures which employ many molecular dynamics steps, often used in the production of glassy polymer structures.[55] Fortunately, unlike porous polymers,[60] achieving an equilibrated amorphous PMM system can be relatively straightforward owing to the smaller size and structural rigidity which affords fewer relevant degrees of freedom. Fig. 5 outlines the key steps for the simple procedure which has been used to produce a number of structural models of PMMs.[23,61-63] Initially, a random loading step at very low density is performed. This initial configuration is subsequently stabilized by classical molecular dynamics simulations without changing the density, using the (*N*, *V*, *T*) ensemble. Thereafter a series of (*N*, *P*, *T*) simulations are employed to pack the structure to a reasonable density. Notably, this compression step requires significant equilibration, >5 ns, and in some cases many annealing steps,[60] which can be computationally demanding. Thus accelerated simulations using graphical processor units (GPUs) have been employed in the application of this methodology to larger molecular structures.[63]

This molecular simulation methodology has been used to generate the structures for a number of PMMs to predict and understand their pore structure. Abbott *et al.* reported the amorphous structure of 22 organic molecules of intrinsic microporosity[64] (OMIMs) with variations of functionality at the core and periphery (end-groups).[61] The simulations identified a number of structure-property relationships that lead to greater porosity. For example, molecular rigidity, bulky periphery moieties and a 3D structure. Indeed, ideal simulations of OMIM-[2 + 5] employing rigid-body molecules found the amorphous phase exhibited a surface area an order of magnitude larger than that observed using flexible-molecule simulations, thus highlighting the importance of molecular rigidity. The design principles examined here for OMIMs are also applicable to other PMMs such as porous organic cages. To this end, Jiang and coworkers have investigated the amorphous packing of **CC3** derivatives.[23,62] These studies showed that increased porosity in the amorphous phase, compared to their crystalline counterparts, results from an increase in inter-cage void volume. This additional porosity more than compensates for the loss in accessible internal cage volume caused by disrupting the ordered channels connecting the cage voids. Moreover, Jiang *et al.* were able to demonstrate connectivity of the extrinsic voids and simulate the diffusion of gases within the pore structure.[62] It is noteworthy that this amorphous phase exhibited high gas selectivity for H_2/N_2, which was rationalized due to a transient

interconnected pore structure. Subsequently, the simulation of larger porous cage structures were performed by Evans *et al*.[63] These studies were made possible by GPU-accelerated molecular dynamics simulations. Nine cage systems were investigated, including two hypothetical structures. The outcome of this work was that key relationships between structure and porosity were identified that mirrored those of Abbott *et al*. However, a novel finding was that cage geometry is a crucial property for bulk porosity. It was uncovered that certain cages could interdigitate and consequently produce dense amorphous networks with unremarkable pore volume, despite the large internal volume and cage size. The use of simulation is particularly useful for such cases where the structure packing is not intuitive.

Importantly, the simulations described above show good agreement to empirical data, including gas adsorption.[23,64] Accordingly, simulations can be viewed as an essential tool for atomistic understanding of the properties of amorphous materials, such as the origin of porosity, that are not easily unobtainable by experimental methods alone.

2.3 Liquid phase

The discrete molecular nature of PMMs affords the possibility to generate liquids of permanent porosity. Porous liquids were initially a hypothetical concept.[65] However, recently, experimental evidence of these novel materials has been demonstrated.[18,66,67] This now burgeoning area of materials science[68] will undoubtedly benefit from the application of computer simulation.

The largely unexplored area of porous liquids used computer simulations as a starting point to design and estimate the properties of liquids based on cage molecules.[69] By functionalising the periphery of these molecules with hydrocarbon moieties, the melting point of the bulk material can be significantly reduced, from above 573 K to 313 K. Simulations were carried out on hypothetical cage materials with surfaces decorated by hydrocarbon chains of varied length and substituents to evaluate their physical properties. In a similar approach to amorphous structure simulations, liquid simulations begin with randomly arranging a number of molecules In a periodic box followed by a high temperature equilibration step and extensive annealing to approximately 200 K using molecular dynamics simulations. Analysis of the annealing trajectories can reveal a wealth of thermodynamic information, including melting points. In tandem with experimental observations,[66] the simulations confirm that increasing chain length significantly decreases the melting point. Additionally, the molecular-level picture available from atomistic simulations can provide an understanding of the nature of porosity in these cavity-based liquid systems. Although, long unbranched chains facilitate low melting points, they can also enter cage cavities as delineated in Fig. 6, and as a result decrease the available void space and hence the potential for permanent porosity. To avoid this issue,

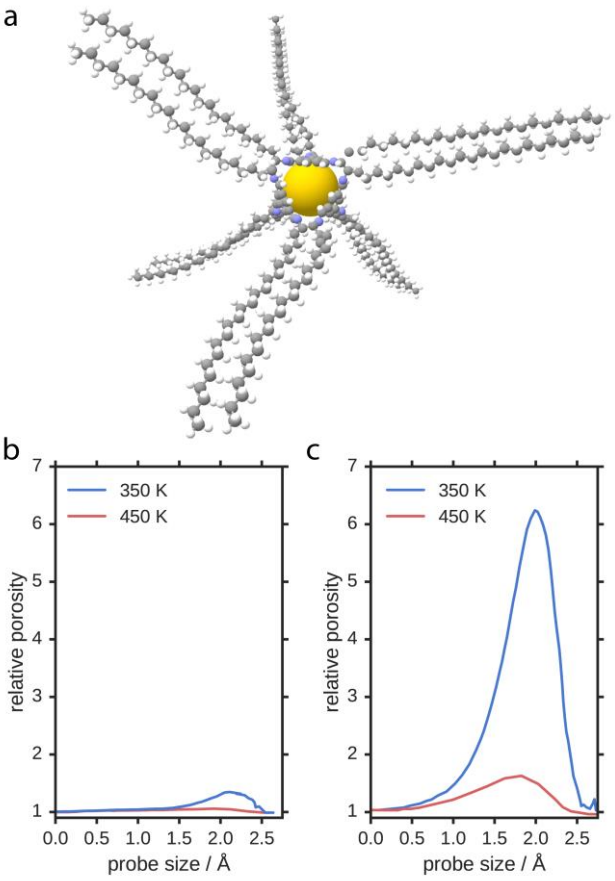

Fig. 6 (a) Structure of an organic cage substituted with C_{22} functionality, which is observed as a liquid at room temperature. Relative porosity observed for (b) C_{12} and (c) C_{14}-neo functionalised cages showing that bulky terminal groups which are unable to penetrate into the molecular cage cavity results in increased porosity of the liquid. Adapted from reference 69.

functional groups must be chosen such that they are unable to penetrate into the molecular cage cavities. Ultimately, these results led to design principles that inspired the synthesis of crown-ether functionalized cages which exhibit a methane solubility of 52 µmol g^{-1} at 303 K.[18] Detailed classical molecular dynamics simulation, in tandem to Positron (e+) Annihilation Lifetime Spectroscopy (PALS), confirmed that this remarkable solubility is attributed to the presence of porous cavities in the liquid and not simple solvating effects of the aromatic cage structure.

3. Porosity, Adsorption and Kinetics

The supramolecular construction of PMMs gives rise to dynamic and potentially constrictive pore structures that have been shown to be favourable for some gas separations. For example, **CC3** (Figure 2c) has demonstrated exceptional potential for noble gas and enantioselective separations.[70] This dynamic behavior has required novel computational approaches to successfully comprehend the selectivity observed in these materials.

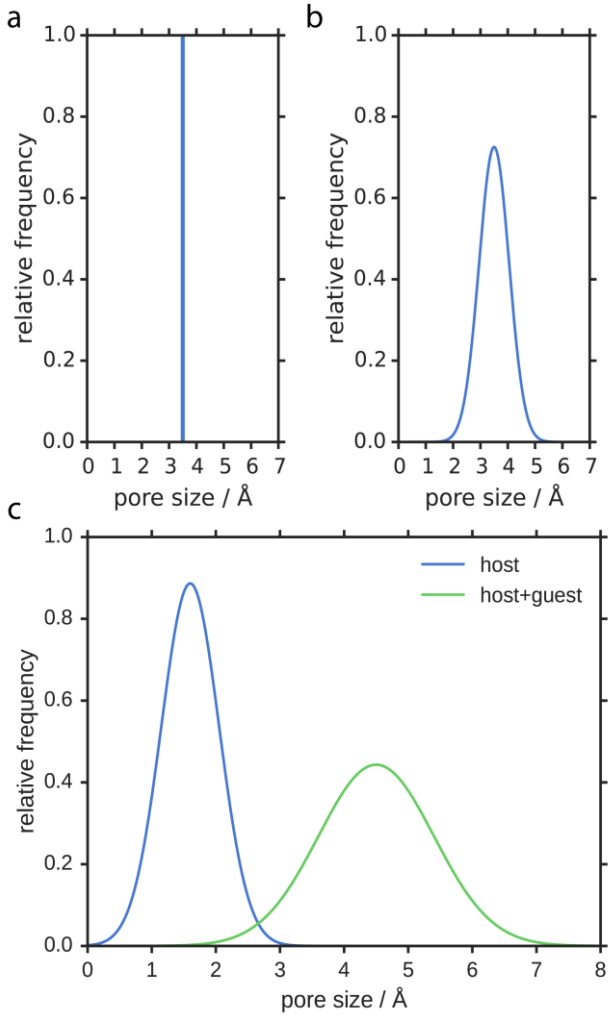

Fig. 7 Illustrative distributions of pore size demonstrating the three classes of dynamic porosity observed in PMMs: (a) static porosity, (b) dynamic porosity and (c) cooperative porosity.

3.1 Dynamic porosity

Whilst there has been substantial success in calculating gas sorption in PMMs assuming a simple rigid host approximation, this is not always the case where there are significant effects from host dynamic behaviour. The influence of the dynamic motion of the host material can influence gas uptake and diffusion in porous network materials such as zeolites and MOFs.[71] This is often exasperated for PMMs, where there is an absence of strong directional bonding between the molecular building slots and pore size is often comparatively small or of similar size to that of guest sorbates. Indeed, the excellent separation performance reported for some PMMs often results from the close match in size and/or shape of the sorbates and the PMMs cavities or limiting pore diameter. Consideration of host dynamic motion can be vital in understanding how pores become interconnected to allow sorbate diffusion, explaining the phenomenon termed by Barbour as "porosity without pores".[72]

A phase transition in a porous material in response to an external stimulus such as pressure or guest sorption could cause a change in sorption properties, equivalent to the well-known breathing behaviour of the MOF, MIL-53.[73] This large scale rearrangement of molecular building blocks and crystal lattice is challenging to computationally predict, and this has not yet been reported for PMMs. However, CSP techniques can identify additional polymorphs lying close in energy, and therefore hypothetically accessible, and solvent stabilisation effects on hypothetical polymorphs assessed in an attempt to identify solvents that can stabilise a given structure. This could be beneficial if predictive, for example identifying how dioxane can help direct to diamondoid pore structures in some porous imine cage systems.[74]

As defined by Holden *et al.*,[75] there are three classes of effects to consider when exploring host flexibility in these systems, Fig. 7. Firstly, a system that requires no consideration of host flexibility can be termed as having 'static porosity'; whereas 'dynamic porosity' refers to pore interconnectivity that occurs through motions of the host even when empty (not loaded with guest). Finally, 'cooperative porosity' refers to systems where the guest influences the host to allow pore interconnectivity that would not occur in the absence of the guest. Crystallography can provide only averaged information on the host positions and therefore for both dynamic and cooperative porosity, simulations can provide insight into fluctuant pore interconnectivity that is not possible through experiment alone.

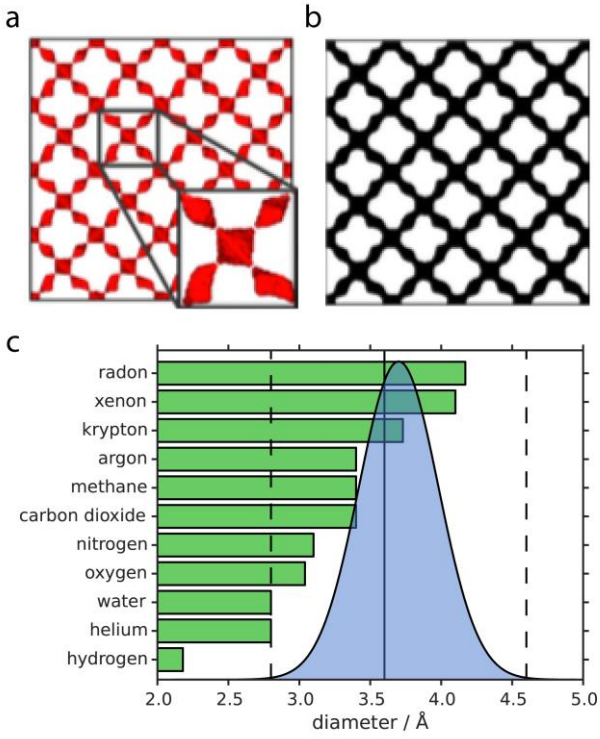

Fig. 8 Comparison of dynamic pore connectivity using the void space histogram approach for (a) rigid and (b) flexible MD simulations with a probe diameter corresponding to Kr in **CC3**. The isosurfaces illustrated correspond to the pore volume accessible for 0.1 ns (10%) of a 1 ns MD simulation. The rigid simulation (inset) shows a disconnected the void space at the window sites. (c) Further MD simulations (298 K, 1 atm) demonstrate the pore-limiting envelope (blue) exhibited by CC3. This pore structure allows diffusion of all rare gases up to radon. The vertical dashed lines indicate the low and high limits of this pore-limiting envelope. The straight, vertical line corresponds to the pore-limiting diameter measured from the static crystal structure at 173 K. Reproduced from Ref. 76 with permission from the American Chemical Society, copyright 2014 and adapted from Ref. 70, respectively.

Jiang *et al.* found evidence of transient void interconnectivity for configurations of amorphous systems loaded with N_2 molecules sampled from different steps in an MD simulation.[62] Holden *et al.* subsequently developed an approach to analyse dynamic pore interconnectivity through sampling MD configurations of empty porous imine cage systems, displayed in Fig. 8.[76] The void space of each configuration was then analysed with respect to a probe to identify void space and interconnected channels in each configuration. Whilst this allowed them to visualise pore opening and closing events, demonstrating dynamic porosity in the systems, the data was also processed further to construct 'void space histograms' that allow one to visualise voids that are open for specific time periods across the entire system, for example voids accessible for at least 100 ps of a 1 ns simulation. These are voids that would appear inaccessible from analysis of the static crystal structure alone. Through focusing on the dynamic variation of the size of the pore neck over time in the MD simulation, this further allows the construction of 'pore limiting envelopes' (PLEs), a histogram of the sampled pore neck sizes. This concept, also used for porous network materials, has been useful in rationalising the diffusion of gases that would seem too large to diffuse based on the pore neck size of the crystal structure, demonstrated in Fig. 8.[70,77]

The dynamic analysis approach has been further used to rationalise dynamic porosity in multicomponent porous imine cage systems[76] and for the porous imine system **CC2**,[78] identifying and distinguishing both dynamic and cooperative porosity effects. This has identified some limits in what can be deduced with certainty from these simulations, in particular with respect to rare diffusion events. For example, in **CC2**, PXRD demonstrated that Xe was located in formally isolated voids within the system. However, the simulations did not find these voids to be interconnected to the main channel network at any point. It was therefore the combination of experimental and simulation information that allowed deduction of a cooperative porosity effect, whereby Xe promotes channel opening. These Xe hopping events were not observed in MD simulations with **CC2** loaded with Xe, presumably due to them being rare events that did not occur on the accessible MD timescales. In section 3.3, we will discuss in further detail computational approaches that can be used to sample such rare diffusion events.

3.2 Gas Adsorption

Similar to conventional porous materials, such as zeolites and MOFs,[79] adsorption of guests in PMMs is simulated using Monte Carlo methods.[80] This technique was used to demonstrate the applicability of BET analysis for determining surface areas in framework materials.[81] Alternatively, electronic structure simulations can be used to investigate local guest-host interactions.[82]

Grand canonical Monte Carlo (GCMC) simulations have been used to simulate full adsorption isotherms from using atom-atom model potentials. These simulations produce isotherms that can be compared to experimental results, but can also highlight favourable adsorption sites.[12,83-85] However, as previously mentioned, PMMs exhibit significant structural flexibility and as a result the accuracy of conventional Monte Carlo simulations may be compromised.[86] GCMC typically treats the porous material as a rigid structure, accordingly, any dynamic porosity or structural responses (such as swelling) in response to guest molecules is ignored. While this approach gives an accurate representation of conventional porous materials (e.g MOFs) it is not necessarily appropriate for PMMs. For example, GCMC simulations of gas adsorption in 1,3,5,2,4,6-triazatriphosphinine using carefully generated potentials showed good accuracy for CO_2 at 195 K, as illustrated in Fig. 9, however, there was significant overestimation at elevated temperatures and for N_2, CH_4 and Xe gases.[84] There are a number of computational routes to simulate gas sorption for soft materials that undergo phase transitions,[87] though we note these approaches have only been applied to a limited number of materials.[88,89] In spite of the challenges outlined here, these simulations have still been useful in predicting and understanding gas adsorption

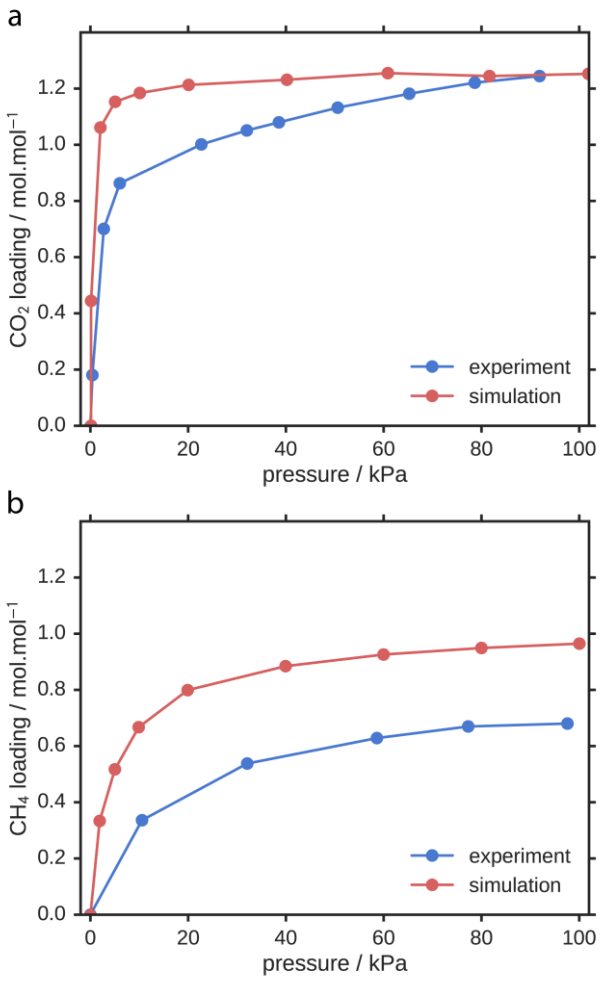

Fig. 9 Comparison of GCMC simulation and experimental observations of (a) CO_2 and (b) CH_4 adsorption at 195 K for 1,3,5,2,4,6-triazatriphosphinine. Adapted from reference 84.

properties.

Gas adsorption simulations primarily use atom-atom model potentials to describe adsorbate-adsorbent interactions, however, high level *ab initio* and density functional theory (DFT) simulations have also been employed. This can be simply for characterising the interaction energy between the material and the gas[82] or to generate tailored model potentials for GCMC simulations.[84] A unique approach was recently applied by Barbour and coworkers.[90] Three states, were modeled using DFT simulations; an empty metallocycle, a metallocycle with one guest and a metallocycle with two guests (the maximum occupancy). The resulting interaction energies, obtained from these simulations, were used to construct of a statistical model to give total occupancy as a function of pressure. This simple model was used to reveal the atomistic mechanism resulting in the observed inflection in an acetylene adsorption isotherm.

3.3 Gas Diffusion

Classical molecular dynamics (MD) simulations are commonly used to chart the diffusion of gases or even larger guests in porous materials.[91,92] MD simulations can, in a straightforward approach, include the dynamic nature of the material. In particular simulations which give kinetic information of adsorbate diffusion is a crucial assessment for PMMs, as many exhibit the aforementioned phenomenon of "porosity without pores".[72]

These simulations proved vital to understanding the accessible porosity of p-tert-butylcalix[4]arene (tBC) to a wide variety of guests. Initial MD simulations explored the inclusion energy of H_2, CH_4, CO_2 and Xe within tBC in an effort to understand the relative retention of these gases.[93] A later investigation used a fully flexible model of tBC to understand the mechanism for the empirically observed H_2 diffusion.[94] However, longer simulations to obtain a diffusion coefficient were not performed. For the larger, less constrained, pore structures of molecular cages MD simulations have been employed to chart the diffusion of a wide variety gases and larger guest molecules.[70,77,95] Furthermore, by combining the GCMC adsorption and MD diffusion simulations, the permeability of a material can be simulated.[96] This is an important consideration when examining a material for gas separation applications.[97] To this end the permeability of several molecular cage materials (combined with typical polymer supports) were predicted and expected to perform well for H_2/CO_2 separations.[77]

The simulation of diffusion in materials with constricted pores is less straightforward, especially for large species where diffusion is a rare event and thus cannot be statistically observed by MD simulations.[98] We note that to obtain a well-converged value of diffusivity, hundreds of diffusion events must be observed. This is a significant challenge for simulating diffusion in nanoporous materials.[99] Constrained dynamics and metadynamics are powerful methods used to examine properties, such as diffusivity and free energy profiles, for these rare events.[100] For example, metadynamics has been employed to understand the concerted mechanism by which hydrogen-bond networks reorganize in Dianin's compound;[101] a key mechanism for gas diffusion in this formally non-porous structure. Recently, Camp and Sholl have described the application of transition state theory to measure the diffusion of large adsorbates in **CC3**.[102] Implicit ligand sampling and umbrella sampling calculations[103,104] were shown to agree with costly direct MD simulation. Moreover, in this work, the efficiency of such methods is illustrated. Less than 3 ns of MD simulations were needed to measure the diffusivity of SF_6 by umbrella sampling, where, in contrast, 1000 ns of MD simulation is required to measure the diffusivity of this slow adsorbate by conventional sampling methods.

Porous liquids, as described in Section 2.3, are an exciting new class of material and there are already efforts to use molecular simulations to understand the complex gas adsorption processes. Qiao and coworkers have employed simulations to describe the thermodynamics and kinetics for the storage of N_2, CO_2 and CH_4 molecules in porous liquids consisting of crown-ether functionalised cage molecules in a 15-crown-5 solvent.[105] Classical MD simulations revealed the characteristics of gas diffusion in the liquid. Notably, the gas storage capacity here relates to a trade-off between cage affinity for gases and accommodation of gases within the cage cavity. This evokes an intrinsic gas storage capacity of CH_4 > CO_2 > N_2. Moreover, by calculating the potential of mean force[106] of the gas molecules, the kinetics of molecules entering and leaving the cage cavity can be predicted. A modest energy penalty for gases leaving the cage cavity was uncovered. The atomistic insight provided by this study resulted in rational design rules for the production of porous liquids and their application.

4. Design and Screening

The extensive body of work relating to the computational analysis of porous framework materials[107-109] has given rise to *a priori* design[110] and high-throughput screening.[111]

4.1 Computational Design

If one considers only small organic molecules as potential extrinsically PMMs or as building blocks for intrinsically PMMs, then there are already an estimated 10^{60} candidates. With combinations of these forming intrinsically PMMs, the search space is even larger. The approach for extrinsically PMMs, involving screening with CSP has already been discussed, and so here we focus on intrinsically PMMs. Given a candidate intrinsically PMM, one might again perform CSP to predict the likely crystal structure or possible polymorphs and to characterise the system further with solid state simulations. However, in some cases it has been shown that molecular simulations on the single molecule alone can be used to

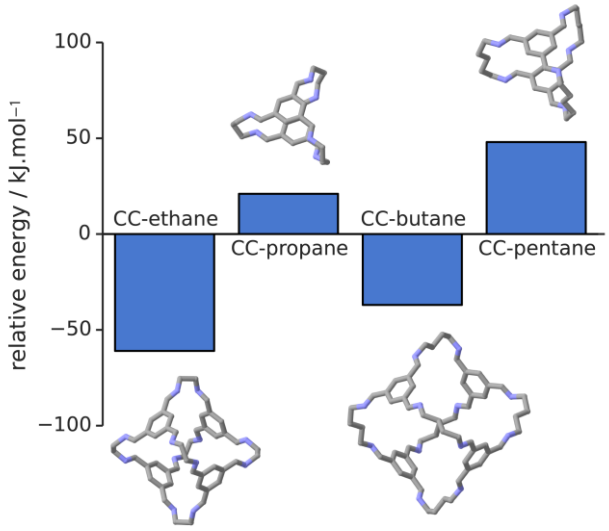

Fig. 10 Alternation of cage molecular mass with increasing alkane chain length component as predicted by calculations in agreement with experiment . The energy is the optimized DFT energy of the [4+6] cage relative to the [2+3] cage structure.

predict solid state or solution properties, in particular separation[112] and sensing performance.[113] Although effects resulting from bulk structure can be expected to influence performance, simulations at the molecular level can be performed considerably quicker and thus allow a preliminary screening to narrow down the number of candidates.

The vast majority of intrinsically PMMs reported to date are synthesised through the use of dynamic covalent chemistry, for example imine condensation reactions. These reactions are reversible and there is therefore an opportunity of forming the thermodynamic product of the reaction. However, there can be multiple possible reaction outcomes in terms of the topology formed, with options including small capsules, tetrahedra, octahedra and cuboctahedra. In some cases the topology can be designed by chemical intuition, but there are also reports of emergent behaviour thwarting this, where small changes in the precursor have had a large effect on both topology and properties.[114] The fact that the thermodynamic product should dominate opens the possibility of comparing the relative energies of low energy conformations of different topological outcomes, typically using electronic structure calculations. This approach has predicted, for example, odd-even alternation in topology with increasing alkane chain length of precursors, illustrated in Fig. 10.[115] There are likely limitations to this approach, in particular due to the difficulty of including the effect of solvent choice,[116] which is known to influence topology in some cases.[117] Further, if targeting a specific topology, the accurate quantification of strain or formation energy is challenging for small organic molecules, let alone these, typically large, systems. However, if success levels greater than chemical intuition alone can be achieved, in the future this approach is likely to see success moving beyond the examples of post-synthetic rationalisation to prediction of promising synthetic targets.

4.2 Screening

Combined chemical intuition and computational design have been responsible for many crucial developments in the field of PMMs. Recently, with increasing computational power and advances in simulation efficiency, there have many reports of high-throughput computational screening studies aimed at identifying new porous structures and uncovering important structure–property relationships.[118] High-throughput simulation methods are relatively well developed for conventional porous materials and have thus facilitated this approach to the field of PMMs.

The benefits of applying screening methods to PMMs was shown by McKeown *et al.*, who uncovered a previously unrealised porous solid from a targeted search of the

Table 1 A selection of CSD codes of crystalline PMM candidates identified by Mckown (top) and Evans (bottom) shown with density, limiting pore diameter and void fraction (ρ, LPD and void fraction for a 1.3 Å probe size). * labels structures which have been experimentally verified as porous.

structure	ρ / g.cm^{-3}	LPD / Å	void fraction
ABINOP	0.765356	11.17951	0.21472
BALNIM*	0.830425	4.03738	0.073
EFALEC	0.641375	13.11797	0.40442
FAKTIV	0.927143	4.13204	0.13068
GIPTOO	0.636011	7.79066	0.28498
KETYEO	1.65289	1.04887	0
NASQAA	0.842207	4.24878	0.0902
PETREM	1.3324	1.26271	0
RERNEI*	0.6925	7.79951	0.23418
SULDUY	0.882964	4.97740	0.12942
TOZZIR	0.621795	12.08235	0.4226
WAVJAE	1.66859	1.17875	0
XICRUW	0.805468	4.71231	0.10504
XOPYEG	0.648454	6.40991	0.41704
YUPTIM	1.15414	1.56534	0
ADIYIV	1.13566	5.16212	0.1556
FOSTEM	0.915622	4.87005	0.06338
FOSTEM10	0.915622	4.87005	0.06338
GOBSUL	0.972968	1.80740	0.00084
IKANOX	0.879286	5.32264	0.12874
KISYIV	0.14872	17.78556	0.8394
TIKFIC	0.896599	3.52835	0.1076
FEQXAC*	0.555444	4.88522	0.32572
GIPCAJ	0.593533	8.17138	0.33668
DIHGOR	0.763993	7.64503	0.3151
MAVSIL	0.97004	5.82261	0.1658
TADWAY	0.829491	5.49993	0.15602
CXPMSO01	1.27681	5.77024	0.0471
ZEXRIF02	0.836306	5.18550	0.13684
VEWGOT	0.932767	1.67450	0.0542
ZEXRIF	0.88807	4.77464	0.137
RIYQEW	1.21265	4.57990	0.15244

Cambridge Structural Database (CSD).[119] This was achieved by considering structures with a density of less than 0.9 g.cm^{-3}, as many crystalline PMMs exhibit low density. These set of structures was further reduced by rejecting molecules composed predominantly of saturated hydrocarbons and inorganic components, which provide structures of low density but are nonporous. The remaining organic structures were further reduced by eliminating those with pores of diameter greater than 10 Å, as they exhibited questionable values for density or had dubious structural parameters as identified by the checkCIF program. This process led to the set of structures shown in Table 1. Among these potential PMM candidates was the structure tetra(trimethylsilylethynyl)biphenyl,[120] which demonstrated, experimentally, a previously unobserved BET surface area of 278 m^2.g^{-1}.

Inspired by the work of McKeown and coworkers, a similar approach was applied by Mastalerz *et al*. By studying structures deposited in the CSD that form flat ordered sheets it was discovered that benzimidazolones showed potential for the construction of extrinsic porous crystalline materials with one-dimensional channels. This ultimately lead to the synthesis of a rigid triptycene-based molecule that self-assembled via hydrogen bonds to a permanently porous crystal with one-dimensional channels of a diameter of 14 Å and a BET surface area of 2796 m^2.g^{-1}. [47]

Recently, motivated by the advances in efficiency of screening conventional porous materials,[121] Evans and coworkers reported a screening of the CSD for porosity.[30] This investigation used geometry-based analysis and molecular simulations to screen the porosity of over 150000 organic molecular crystal structures. 481 potential organic porous molecular crystals were identified and the surface area and pore dimensions of these structures were computed, with notable examples displayed in Table 1. Furthermore, Fig. 11 illustrates the volumetric surface areas of the identified organic PMMs compared to the databases of zeolites and MOFs highlighting the unique porosity exhibited by these systems. Importantly, this computer-generated database has been used to uncover a number of trends and properties that had not previously been quantified due to the limited number of reported PMMs. Using machine learning, it was shown that the van der Waals surface area (quantified by the labuteASA value[122]), and other related descriptors of molecular size, are the molecular properties best able to predict the propensity for a crystal to form structural voids.

5. Conclusion and Outlook

Computational methods have proved to be crucial to the development of PMMs. Here we have outlined approaches for the production of atomistic models, porosity analysis and the simulation of gas adsorption and diffusion. Furthermore, we have highlighted examples where these methods have been used for the *a priori* design and large scale screening of candidate PMMs. While many of these computational approaches have been employed to investigate porous framework and polymer materials,[60,79] the discrete

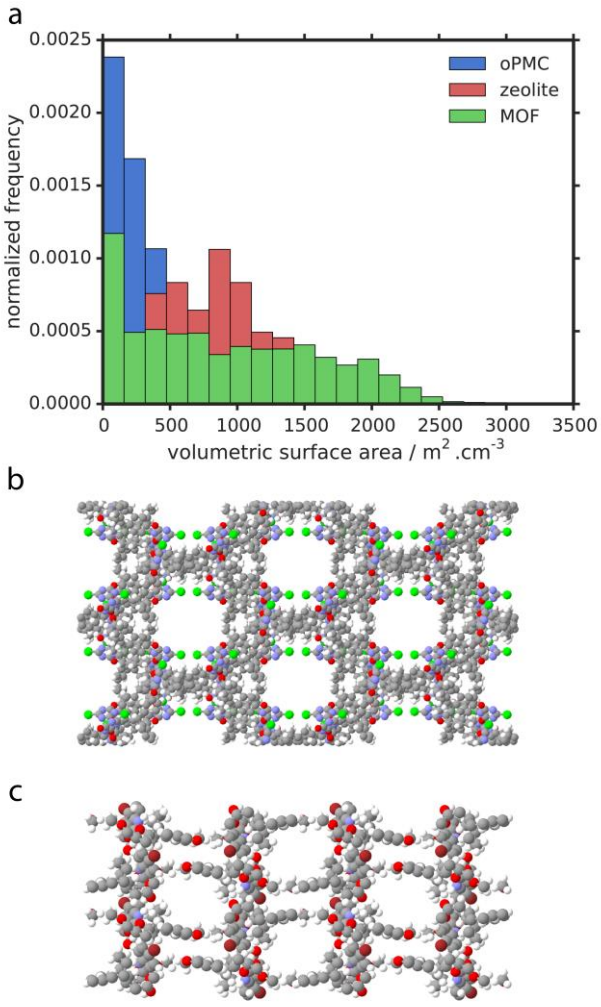

Fig. 11 (a) The distribution of volumetric surface area observed for organic crystalline PPMs (oPMC), zeolites and MOFs. Crystal structures of (b) DIHGOR and (c) MAVSIL (CSD codes) which have been identified as candidates for new PMMs.

composition and disconnected pores typical of PMMs has necessitated the development of novel methodologies. Salient examples are the analysis of dynamic pore interconnectivity[76] and the use of transition state theory to inspect the diffusion of large and constrained adsorbates.[102] We note that the development of novel computational methods for PMMs are readily applicable to other challenging dynamic porous materials.[71]

Recent investigations have demonstrated how molecular simulations will help shape future research in the field of PMMs. Advances in crystal structure prediction[20] and high-throughput screening methods[123] suggest that computational 'mining' of databases will uncover a library of new materials to study. Furthermore, the increased accuracy of gas adsorption and diffusion simulations will facilitate *in silico* screening of a materials performance characteristics for a desired application. Additionally, the research described here is primarily directed towards organic materials. There are

however many metal—organic PMMs[124] for which the structures and properties can be elucidated by computational methods. Whereas the organic structures are well described by model potentials, flexible metal—organic moieties require careful parameterisation which has inhibited analogous studies. Accurate and efficient descriptions of metal clusters is beginning to be addressed in framework materials[125] and it is anticipated that these methods could be extended to PMMs.

Although the field of computational simulations of PMMs has advanced significantly in recent years, a number of challenges remain. For example, the effect of solvent, which has been shown to influence the resulting PMM local and periodic structure need to be addressed.[116] Nevertheless, PMMs are a rapidly growing field and the computational strategies outlined herein will continue to play a vital role in the design, characterisation and exploration of novel applications.

Acknowledgements

JDE thanks Dr François-Xavier Coudert and the PSL Research University for funding (project DEFORM, grant ANR-10-IDEX-0001-02). GMD thanks the European Research Council under the European Union's Seventh Framework Programme (FP/2007-2013)/ERC through grant agreement n. 307358 (ERC-stG-2012-ANGLE) and the EPSRC (grant EP/K018132/1), KEJ acknowledges the Royal Society for a University Research Fellowship.

Notes and references

1 M. E. Davis, *Nature*, 2002, **417**, 813–821.
2 H. Furukawa, K. E. Cordova, M. O'Keeffe and O. M. Yaghi, *Science*, 2013, **341**, 1230444–1230444.
3 D. S. Sholl and R. P. Lively, *Nature*, 2016, **532**, 435–437.
4 N. Mizuno and M. Misono, *Chem. Rev.*, 1998, **98**, 199–218.
5 A. Corma, *Chem. Rev.*, 1997, **97**, 2373–2420.
6 J. Lee, J. Kim and T. Hyeon, *Adv. Mater.*, 2006, **18**, 2073–2094.
7 N. McKeown, *J. Mater. Chem.*, 2010, **20**, 10588-10597.
8 J. Tian, P. K. Thallapally and B. P. McGrail, *CrystEngComm*, 2012, **14**, 1909–1919.
9 T. Hasell and A. I. Cooper, *Nat. Rev. Mater.*, 2016, **1**, 16053.
10 R. M. Barrer and V. H. Shanson, *J. Chem. Soc. Chem. Commun.*, 1976, 333–334.
11 S. A. Allison and R. M. Barrer, *J. Chem. Soc. A*, 1969, 1717-1723.
12 T. Tozawa, J. T. A. Jones, S. I. Swamy, S. Jiang, D. J. Adams, S. Shakespeare, R. Clowes, D. Bradshaw, T. Hasell, S. Y. Chong, C. Tang, S. Thompson, J. Parker, A. Trewin, J. Bacsa, A. M. Z. Slawin, A. Steiner and A. I. Cooper, *Nat. Mater.*, 2009, **8**, 973–978.
13 M. Kitchin, J. Teo, K. Konstas, C. H. Lau, C. J. Sumby, A. W. Thornton, C. J. Doonan and M. R. Hill, *J. Mater. Chem. A*, 2015, **3**, 15241-15247
14 A. F. Bushell, P. M. Budd, M. P. Attfield, J. T. A. Jones, T. Hasell, A. I. Cooper, P. Bernardo, F. Bazzarelli, G. Clarizia and J. C. Jansen, *Angew. Chem., Int. Ed.,* 2012, **52**, 1253–1256
15 T. Hasell, S. Y. Chong, M. Schmidtmann, D. J. Adams and A. I. Cooper, *Angew. Chem., Int. Ed*., 2012, **51**, 7154-7157
16 G. Zhang, O. Presly, F. White, I. M. Oppel and M. Mastalerz, *Angew. Chem., Int. Ed.*, 2014, **53**, 1516–1520.
17 T. Hasell, S. Y. Chong, K. E. Jelfs, D. J. Adams and A. I. Cooper, *J. Am. Chem. Soc.*, 2012, **134**, 588–598.
18 N. Giri, M. G. Del Pópolo, G. Melaugh, R. L. Greenaway, K. Rätzke, T. Koschine, L. Pison, M. F. C. Gomes, A. I. Cooper and S. L. James, *Nature*, 2015, **527**, 216–220.
19 J. Nyman and G. M. Day, *CrystEngComm*, 2015, **17**, 5154–5165.
20 E. O. Pyzer-Knapp, H. P. G. Thompson, F. Schiffmann, K. E. Jelfs, S. Y. Chong, M. A. Little, A. I. Cooper and G. M. Day, *Chem. Sci.*, 2014, **5**, 2235–2245.
21 O. M. Yaghi, M. O'Keeffe, N. W. Ockwig, H. K. Chae, M. Eddaoudi and J. Kim, *Nature*, 2003, **423**, 705–714.
22 A. G. Slater, M. A. Little, A. Pulido, S. Y. Chong, D. Holden, L. Chen, C. Morgan, X. Wu, G. Cheng, R. Clowes, M. E. Briggs, T. Hasell, K. E. Jelfs, G. M. Day and A. I. Cooper, *Nat. Chem.*, 2017, **9**, 17–25.
23 S. Jiang, J. T. A. Jones, T. Hasell, C. E. Blythe, D. J. Adams, A. Trewin and A. I. Cooper, *Nat. Commun.*, 2011, **2**, 207.
24 S. O. Odoh, C. J. Cramer, D. G. Truhlar and L. Gagliardi, *Chem. Rev.*, 2015, **115**, 6051–6111.
25 M. A. Neumann and M.-A. Perrin, *J. Phys. Chem. B*, 2005, **109**, 15531–15541.
26 J. Hermann, R. A. DiStasio Jr. and A. Tkatchenko, *Chem. Rev.*, 2017, **117**, 4714–4758.
27 D. Frenkel and B. Smit, *Understanding molecular simulations: from algorithms to applications*, Academic, 1996.
28 J. Nyman, O. S. Pundyke and G. M. Day, *Phys. Chem. Chem. Phys.*, 2016, **18**, 15828–15837.
29 D. Holden, K. E. Jelfs, A. I. Cooper, A. Trewin and D. J. Willock, *J. Phys. Chem. C*, 2012, **116**, 16639–16651.
30 J. D. Evans, D. M. Huang, M. Haranczyk, A. W. Thornton, C. J. Sumby and C. J. Doonan, *CrystEngComm*, 2016, **18**, 4133–4141.
31 J. T. A. Jones, T. Hasell, X. Wu, J. Bacsa, K. E. Jelfs, M. Schmidtmann, S. Y. Chong, D. J. Adams, A. Trewin, F. Schiffman, F. Cora, B. Slater, A. Steiner, G. M. Day and A. I. Cooper, *Nature*, 2011, **474**, 367–371.
32 A. Pulido, L. Chen, T. Kaczorowski, D. Holden, M. A. Little, S. Y. Chong, B. J. Slater, D. P. McMahon, B. Bonillo, C. J. Stackhouse, A. Stephenson, C. M. Kane, R. Clowes, T. Hasell, A. I. Cooper and G. M. Day, *Nature*, 2017, **543**, 657-664
33 S. M. Woodley and R. Catlow, *Nat. Mater.*, 2008, **7**, 937–946.
34 G. M. Day, *Crystallog. Rev.*, 2011, **17**, 3–52.
35 D. H. Case, J. E. Campbell, P. J. Bygrave and G. M. Day, *J. Chem. Theory Comput.*, 2016, **12**, 910–924.
36 G. M. Day, T. G. Cooper, A. J. Cruz-Cabeza, K. E. Hejczyk, H. L. Ammon, S. X. M. Boerrigter, J. S. Tan, R. G. Della Valle, E. Venuti, J. Jose, S. R. Gadre, G. R. Desiraju, T. S. Thakur, B. P. van Eijck, J. C. Facelli, V. E. Bazterra, M. B. Ferraro, D. W. M. Hofmann, M. A. Neumann, F. J. J. Leusen, J. Kendrick, S. L. Price, A. J. Misquitta, P. G. Karamertzanis, G. W. A. Welch, H. A. Scheraga, Y. A. Arnautova, M. U. Schmidt, J. van de Streek, A. K. Wolf, B. Schweizer, *Acta Crystallogr., Sect. B: Struct. Sci., Cryst. Eng. Mater.*, 2009, **65**, 107–125.

37 A. Graeme M Day and W. D. S. Motherwell, *Cryst. Growth Des.*, 2006, **6**, 1985–1990.

38 G. M. Day, W. D. S. Motherwell, H. L. Ammon, S. X. M. Boerrigter, R. G. Della Valle, E. Venuti, A. Dzyabchenko, J. D. Dunitz, B. Schweizer, B. P. van Eijck, P. Erk, J. C. Facelli, V. E. Bazterra, M. B. Ferraro, D. W. M. Hofmann, F. J. J. Leusen, C. Liang, C. C. Pantelides, P. G. Karamertzanis, S. L. Price, T. C. Lewis, H. Nowell, A. Torrisi, H. A. Scheraga, Y. A. Arnautova, M. U. Schmidt, P. Verwer, *Acta Crystallogr., Sect. B: Struct. Sci., Cryst. Eng. Mater.*, 2005, **61**, 511–527.

39 S. L. Price, *Chem. Soc. Rev.*, 2014, **43**, 2098–2111.

40 M. A. Neumann, F. J. J. Leusen and J. Kendrick, *Angew. Chem. Int. Ed. Engl.*, 2008, **47**, 2427–2430.

41 Y. N. Heit, G. J. O. Beran, *Acta Crystallogr., Sect. B: Struct. Crystallogr. Cryst. Chem.*, 2016, **72**, 514–529.

42 A. M. Reilly and A. Tkatchenko, *Phys. Rev. Lett.*, 2014, **113**, 055701.

43 J. Nyman and G. M. Day, *Phys. Chem. Chem. Phys.*, 2016, **18**, 31132–31143.

44 A. J. Cruz Cabeza, G. M. Day, W. D. S. Motherwell and W. Jones, *Chem. Commun.*, 2007, 1600–1602.

45 A. J. Cruz Cabeza, G. M. Day and W. Jones, *Chem.-Eur. J.*, 2009, **15**, 13033–13040.

46 M. Selent, J. Nyman, J. Roukala, M. Ilczyszyn, R. Oilunkaniemi, P. J. Bygrave, R. Laitinen, J. Jokisaari, G. M. Day and P. Lantto, *Chem.-Eur. J.* 2017, 10.1002/chem.201604797

47 M. Mastalerz and I. M. Oppel, *Angew. Chem. Int. Ed. Engl.*, 2012, **51**, 5252–5255.

48 J. Tian, P. K. Thallapally, S. J. Dalgarno, P. B. McGrail and J. L. Atwood, *Angew. Chem., Int. Ed.*, 2009, **48**, 5492-5495.

49 M. W. Schneider, I. M. Oppel, H. Ott, L. G. Lechner, H.-J. S. Hauswald, R. Stoll and M. Mastalerz, *Chem.-Eur. J.*, 2012, **18**, 836–847.

50 W. Paul and G. D. Smith, *Rep. Prog. Phys.*, 2004, **67**, 1117–1185.

51 N. A. Marks, N. C. Cooper, D. R. McKenzie, D. G. McCulloch, P. Bath and S. P. Russo, *Phys. Rev. B*, 2002, **65**, 075411.

52 M. D. Rechtin, A. L. Renninger and B. L. Averbach, *J. Non-Cryst. Solids*, 1974, **15**, 74–82.

53 R. L. McGreevy and L. Pusztai, *Mol. Simul.*, 1988, **1**, 359–367.

54 J. Pikunic, C. Clinard, N. Cohaut, K. E. Gubbins, J.-M. Guet, R. J. M. Pellenq, I. Rannou and J.-N. Rouzaud, *Langmuir*, 2003, **19**, 8565–8582.

55 L. J. Abbott, K. E. Hart and C. M. Colina, *Theor. Chem. Acc.*, 2013, **132**, 1334.

56 J.-C. Liu and P. A. Monson, *Adsorption*, 2005, **11**, 5–13.

57 E. I. Segarra and E. D. Glandt, *Chem. Eng. Sci.*, 1994, **49**, 2953–2965.

58 E. Di Biase and L. Sarkisov, 2013, **64**, 262–280.

59 D. N. Theodorou and U. W. Suter, *Macromolecules*, 1985, **18**, 1467–1478.

60 G. S. Larsen, P. Lin, K. E. Hart and C. M. Colina, *Macromolecules*, 2011, **44**, 6944–6951.

61 L. J. Abbott, N. B. McKeown and C. M. Colina, *J. Mater. Chem. A*, 2013, **1**, 11950.

62 S. Jiang, K. E. Jelfs, D. Holden, T. Hasell, S. Y.-L. Chong, M. Haranczyk, A. Trewin and A. I. Cooper, *J. Am. Chem. Soc.*, 2013, **135**, 17818–17830.

63 J. D. Evans, D. M. Huang, M. R. Hill, C. J. Sumby, D. S. Sholl, A. W. Thornton and C. J. Doonan, *J. Phys. Chem. C*, 2015, **119**, 7746–7754.

64 L. J. Abbott, A. G. McDermott, A. Del Regno, R. G. D. Taylor, C. G. Bezzu, K. J. Msayib, N. B. McKeown, F. R. Siperstein, J. Runt and C. M. Colina, *J. Phys. Chem. B*, 2013, **117**, 355–364.

65 N. O'Reilly, N. Giri and S. L. James, *Chem.-Eur. J.*, 2007, **13**, 3020–3025.

66 N. Giri, C. E. Davidson, G. Melaugh, M. G. Del Pópolo, J. T. A. Jones, T. Hasell, A. I. Cooper, P. N. Horton, M. B. Hursthouse and S. L. James, *Chem. Sci.*, 2012, **3**, 2153.

67 J. Zhang, S.-H. Chai, Z.-A. Qiao, S. M. Mahurin, J. Chen, Y. Fang, S. Wan, K. Nelson, P. Zhang and S. Dai, *Angew. Chem., Int. Ed.*, 2014, **54**, 932–936.

68 S. L. James, *Adv. Mater.*, 2016, **28**, 5712–5716.

69 G. Melaugh, N. Giri, C. E. Davidson, S. L. James and M. G. Del Pópolo, *Phys. Chem. Chem. Phys.*, 2014, **16**, 9422–9431.

70 L. Chen, P. S. Reiss, S. Y. Chong, D. Holden, K. E. Jelfs, T. Hasell, M. A. Little, A. Kewley, M. E. Briggs, A. Stephenson, K. M. Thomas, J. A. Armstrong, J. Bell, J. Busto, R. Noel, J. Liu, D. M. Strachan, P. K. Thallapally and A. I. Cooper, *Nat. Mater.*, 2014, **13**, 954–960.

71 F.-X. Coudert, *Chem. Mater.*, 2015, **27**, 1905–1916.

72 L. J. Barbour, *Chem. Commun.*, 2006, 1163.

73 A. Boutin, M. A. Springuel Huet, A. Nossov, A. Gédéon, T. Loiseau, C. Volkringer, G. Férey, F.-X. Coudert and A. H. Fuchs, *Angew. Chem. Int. Ed. Engl.*, 2009, **48**, 8314–8317.

74 T. Hasell, J. L. Culshaw, S. Y. Chong, M. Schmidtmann, M. A. Little, K. E. Jelfs, E. O. Pyzer-Knapp, H. Shepherd, D. J. Adams, G. M. Day and A. I. Cooper, *J. Am. Chem. Soc.*, 2014, **136**, 1438–1448.

75 D. Holden, S. Y. Chong, L. Chen, K. E. Jelfs, T. Hasell and A. I. Cooper, *Chem. Sci.*, 2016, **7**, 4875–4879.

76 D. Holden, K. E. Jelfs, A. Trewin, D. J. Willock, M. Haranczyk and A. I. Cooper, *J. Phys. Chem. C*, 2014, **118**, 12734–12743.

77 J. D. Evans, D. M. Huang, M. R. Hill, C. J. Sumby, A. W. Thornton and C. J. Doonan, *J. Phys. Chem. C*, 2014, **118**, 1523–1529.

78 R. Manurung, D. Holden, M. Miklitz, L. Chen, T. Hasell, S. Y. Chong, M. Haranczyk, A. I. Cooper and K. E. Jelfs, *J. Phys. Chem. C*, 2015, **119**, 22577–22586.

79 J. D. Evans, G. Fraux, R. Gaillac, D. Kohen, F. Trousselet, J.-M. Vanson and F.-X. Coudert, *Chem. Mater.*, 2017, **29**, 199-212.

80 D. Dubbeldam, A. Torres-Knoop and K. S. Walton, *Mol. Simul.*, 2013, **39**, 1253–1292.

81 K. S. Walton and R. Q. Snurr, *J. Am. Chem. Soc.*, 2007, **129**, 8552–8556.

82 J. M. Teo, C. J. Coghlan, J. D. Evans, E. Tsivion, M. Head-Gordon, C. J. Sumby and C. J. Doonan, *Chem. Commun.*, 2016, **52**, 276–279.

83 W. Li and J. Zhang, *J. Comput. Chem.*, 2014, **35**, 174–180.

84 W. Li, S. Grimme, H. Krieg, J. Möllmann and J. Zhang, *J. Phys. Chem. C*, 2012, **116**, 8865–8871.

85 J. L. Daschbach, X. Sun, P. K. Thallapally, B. P. McGrail and L. X. Dang, *J. Phys. Chem. B*, 2010, **114**, 5764–5768.

86 D. Dubbeldam, S. Calero, D. E. Ellis and R. Q. Snurr, *Mol. Simul.*, 2015, **42**, 81–101.

87 F.-X. Coudert, M. Jeffroy, A. H. Fuchs, A. Boutin and C. Mellot-Draznieks, *J. Am. Chem. Soc.*, 2008, **130**, 14294–14302.

88 D. Bousquet, F. X. Coudert and A. Boutin, *J. Chem. Phys.*, 2012, **137**, 044118..

89 D. Bousquet, F.-X. Coudert, A. G. J. Fossati, A. V. Neimark, A. H. Fuchs and A. Boutin, *J. Chem. Phys.*, 2013, **138**, 174706.

90 T. Jacobs, G. O. Lloyd, J.-A. Gertenbach, K. K. Müller-Nedebock, C. Esterhuysen and L. J. Barbour, *Angew. Chem., Int. Ed.*, 2012, **51**, 4913–4916.

91 R. Krishna, *J. Phys. Chem. C*, 2009, **113**, 19756–19781.

92 D. Dubbeldam and R. Q. Snurr, *Mol. Simul.*, 2007, **33**, 305–325.

93 S. Alavi and J. A. Ripmeester, *Chem.-Eur. J.*, 2008, **14**, 1965–1971.

94 S. Alavi, T. K. Woo, A. Sirjoosingh, S. Lang, I. Moudrakovski and J. A. Ripmeester, *Chem.-Eur. J.*, 2010, **16**, 11689–11696.

95 A. Avellaneda, P. Valente, A. Burgun, J. D. Evans, A. W. Markwell-Heys, D. Rankine, D. J. Nielsen, M. R. Hill, C. J. Sumby and C. J. Doonan, *Angew. Chem., Int. Ed.*, 2013, **52**, 3746–3749.

96 S. Keskin and D. S. Sholl, *Energy Environ. Sci.*, 2010, **3**, 343.

97 B. D. Freeman, *Macromolecules*, 1999, **32**, 375–380.

98 J. Kärger, D. M. Ruthven and D. N. Theodorou, *Diffusion in Nanoporous Materials*, Wiley-VCH Verlag GmbH & Co. KGaA, Weinheim, Germany, 2012.

99 D. Dubbeldam, E. Beerdsen, T. J. H. Vlugt and B. Smit, *J. Chem. Phys.*, 2005, **122**, 224712.

100 A. Laio and F. L. Gervasio, *Rep. Prog. Phys.*, 2008, **71**, 126601.

101 A. Nemkevich, M. A. Spackman and B. Corry, *J. Am. Chem. Soc.*, 2011, **133**, 18880–18888.

102 J. S. Camp and D. S. Sholl, *J. Phys. Chem. C*, 2016, **120**, 1110–1120.

103 J. Cohen, K. W. Olsen and K. Schulten, in *Globins and Other Nitric Oxide-Reactive Proteins, Part B*, Elsevier, 2008, vol. 437, pp. 439–457.

104 P. Virnau and M. Muller, *J. Chem. Phys.*, 2004, **120**, 10925–10930.

105 F. Zhang, F. Yang, J. Huang, B. G. Sumpter and R. Qiao, *J. Phys. Chem. B*, 2016, **120**, 7195–7200.

106 B. Roux, *Comput. Phys. Commun.*, 1995, **91**, 275–282.

107 S. Keskin, J. Liu, R. B. Rankin, J. K. Johnson and D. S. Sholl, *Ind. Eng. Chem. Res.*, 2009, **48**, 2355–2371.

108 T. Düren, Y.-S. Bae and R. Q. Snurr, *Chem. Soc. Rev.*, 2009, **38**, 1237.

109 S. S. Han, J. L. Mendoza-Cortés and W. A. Goddard, *Chem. Soc. Rev.*, 2009, **38**, 1460–1476.

110 O. K. Farha, A. Özgür Yazaydın, I. Eryazici, C. D. Malliakas, B. G. Hauser, M. G. Kanatzidis, S. T. Nguyen, R. Q. Snurr and J. T. Hupp, *Nat. Chem.*, 2010, **2**, 944–948.

111 S. Curtarolo, G. L. W. Hart, M. B. Nardelli, N. Mingo, S. Sanvito and O. Levy, *Nat. Mater.*, 2013, **12**, 191–201.

112 T. Mitra, K. E. Jelfs, M. Schmidtmann, A. Ahmed, S. Y. Chong, D. J. Adams and A. I. Cooper, *Nat. Chem.*, 2013, **5**, 276–281.

113 M. A. Zwijnenburg, E. Berardo, W. J. Peveler and K. E. Jelfs, *J. Phys. Chem. B*, 2016, **120**, 5063–5072.

114 K. E. Jelfs, X. Wu, M. Schmidtmann, J. T. A. Jones, J. E. Warren, D. J. Adams and A. I. Cooper, *Angew. Chem. Int. Ed. Engl.*, 2011, **50**, 10653–10656.

115 K. E. Jelfs, E. G. B. Eden, J. L. Culshaw, S. Shakespeare, E. O. Pyzer-Knapp, H. P. G. Thompson, J. Bacsa, G. M. Day, D. J. Adams and A. I. Cooper, *J. Am. Chem. Soc.*, 2013, **135**, 9307–9310.

116 V. Santolini, G. A. Tribello and K. E. Jelfs, *Chem. Commun.*, 2015, **51**, 15542–15545.

117 X. Liu and R. Warmuth, *J. Am. Chem. Soc.*, 2006, **128**, 14120–14127.

118 Y. J. Colón and R. Q. Snurr, *Chem. Soc. Rev.*, 2014, **43**, 5735–5749.

119 K. J. Msayib, D. Book, P. M. Budd, N. Chaukura, K. D. M. Harris, M. Helliwell, S. Tedds, A. Walton, J. E. Warren, M. Xu and N. B. McKeown, *Angew. Chem. Int. Ed. Engl.*, 2009, **48**, 3273–3277.

120 K. P. U. Perera, M. Krawiec and D. W. Smith Jr., *Tetrahedron*, 2002, **58**, 10197–10203.

121 T. F. Willems, C. H. Rycroft, M. Kazi, J. C. Meza and M. Haranczyk, *Microporous Mesoporous Mater.*, 2012, **149**, 134–141.

122 P. Labute, *J. Mol. Graphics Modell.*, 2000, **18**, 464–477.

123 D. W. Davies, K. T. Butler, A. J. Jackson, A. Morris, J. M. Frost, J. M. Skelton and A. Walsh, *Chem*, 2016, **1**, 617–627.

124 D. J. Tranchemontagne, Z. Ni, M. O'Keeffe and O. M. Yaghi, *Angew. Chem. Int. Ed. Engl.*, 2008, **47**, 5136–5147.

125 S. Bureekaew, S. Amirjalayer, M. Tafipolsky, C. Spickermann, T. K. Roy and R. Schmid, *Phys. Status Solidi B*, 2013, **250**, 1128–1141.